2006 GSTC Proceedings
ASME Graduate Student Technical Conference
April 6 - 8, 2006 – Fayetteville, Arkansas

MODELING OF LIMIT CYCLE THERMOACOUSTIC AND HYDRODYNAMIC BEHAVIOR OF CONICAL CH_4/H_2 FLAMES

Onur Tuncer*
Department of Mechanical
Engineering, Louisiana State
University, Baton Rouge, LA, 70803

ABSTRACT

Premixed gas turbine combustors are susceptible to combustion instabilities, which can yield in hardware damage. Acoustic waves produce oscillations in the unsteady heat release by perturbing the instantaneous equivalence ratio. Furthermore, many land based power generation units currently operate on natural gas many of them need to tackle the challenges due to a fuel switch towards synthesis gas in the near future. Operating conditions of a premixed gas turbine combustor is very sensitive to the changes in the fuel composition.

G-equation is coupled with combustor acoustics in order to track the flame-front, which provides an understanding of dynamic flame holding and flashback behavior. Non-linear relation between acoustic velocity perturbations and equivalence ratio fluctuations is responsible for limit cycle behavior. Assuming a choked fuel injector these equivalence ratio perturbations are traced by seeding the axial airflow with massless particles. It is observed that these particles can cross both the injector and the flame a number of times due to reversal of flow during cycle instability. Behavior of a premixed confined conical hydrogen enriched methane flame is studied with regard to thermo-acoustic instability induced flame flashback and RMS pressure levels over a range of operating conditions.

NOMENCLATURE

A	Cross sectional area / Flame area
C	Mole fraction
c	Speed of sound
D	Combustor diameter
e	Internal energy per unit mass
f	Flame front function
h	Enthalpy of combustion
k	Wave number
L	Flame height / Combustor length
P	Pressure
q	Heat release
S	Flame speed
T	Temperature
t	Time
u	Longitudinal velocity
x	Longitudinal coordinate
z	Axial flame coordinate

Greek Symbols

ϕ	Equivalence ratio
ω	Frequency
α	Thermal diffusivity
Ξ	Set of all times when the particle crosses the injector
γ	Specific heat ratio
δ	Delta function
ρ	Density
ψ	Mode shape

Subscripts

ad	Adiabatic
air	Air
d	Downstream with respect to flame position
f	Flame
fuel	Fuel
in	Inlet
L	Laminar
s	Stoichiometric
u	Upstream with respect to flame position

Superscripts

$\bar{}$	Time average
$(.)'$	Fluctuating quantity
.	Time derivative

INTRODUCTION

Gas turbine engines are commonly utilized in electricity generation. These modern premixed gas turbine combustors are usually operated near the lean blowout limit due to

* Doctoral Candidate, Student Member ASME

emissions considerations [1]. In this operating range flame holding and thermo-acoustic instability become the two most important considerations. Thermo-acoustic instability not only deteriorates the structural integrity of the combustor wall by subjecting it to fatigue loading [2] but also can cause hazardous flashback into the premixing section [3].

Thermo-acoustic oscillations occur because unsteady heating generates sound waves that produce velocity and pressure perturbations. Inside a combustor these oscillations again couple with the heat release [2]. If the unsteady heat input is in phase with pressure perturbations, acoustic waves gain energy and instability becomes possible. In his pioneering work, Lord Rayleigh [4] gives a physical description of this self-excitation phenomenon. In reality, strength of these oscillations are limited by non-linear effects and limit cycle oscillations occur. Exposure to pressure fluctuations may reduce the lifetime of gas turbine hardware. Thermo-acoustic oscillations also have an effect on flame stability and flame holding. During these oscillations flame boundary also moves [5]. Furthermore, the location of the flame-front also affects stability [6]. Should adequate conditions be present flame might enter inside the premixing section triggering flashback. This phenomenon is called thermo-acoustic instability induced flame flashback. For the study of thermo-acoustic instability often the flame is assumed to anchor at a specific point inside the combustor. This assumption is likely to be satisfied in well-stabilized flames, however this paper deals with resolving ill behavior due to poor flame stability. Letting the flame interface move is the only way to study such behavior. On the other hand this approach lacks the fidelity of resolving flame front movement and capturing erratic behavior such as flashback or poor flame holding due to self-excited oscillations.

Synthesis gas is a mixture of primarily hydrogen and carbon monoxide. Energy contribution of syngas in the existing IGCC (integrated gasified combined cycle) land power generation installations is about 10-20% of the total power output. Due to the gasification process substantial change in the resulting syngas composition can occur [7]. The quality and composition of the fuel impacts the turbine life and emissions [8]. Therefore characterization of the flame behavior at different fuel compositions is an extremely important task. In addition, syngas combustion in particular generates many of the necessary conditions for flashback due to high flame speeds associated with its hydrogen content. Therefore, in order to achieve a desired power output from syngas high mass flow rates need to be used since syngas is a low-BTU fuel. High mass flow rates normally require higher injection speeds, which pose a significant problem in terms of flame holding [9].

The aim of this paper is to develop a simple mathematical model for flame holding and thermo-acoustic instability induced type flame flashback in order to understand. Tuncer et. al. [14] developed a similar model but with an ad-hoc closure between the mass flow perturbation input and heat release output by introducing a non-linearity into Annaswamy et. al.'s [10] heat release model which they obtained by linearizing well-stirred-reactor equations. This paper aims to provide a more physically based feedback mechanism to the model and also extend its applicability to blends of multiple fuels such as mixtures of CH_4/H_2, which are investigated within the context of this paper.

MATHEMATICAL MODELING

In this section of the article a mathematical modeling is developed to understand limit cycle hydrodynamic and acoustic behavior of conical confined methane and hydrogen flames. The geometry of the conical flame front is depicted in Figure 1.

Linear Acoustics. Combustor acoustics is governed by the following partial differential equation, which involves a source term in its right hand side at the location of the flame interface due to combustion.

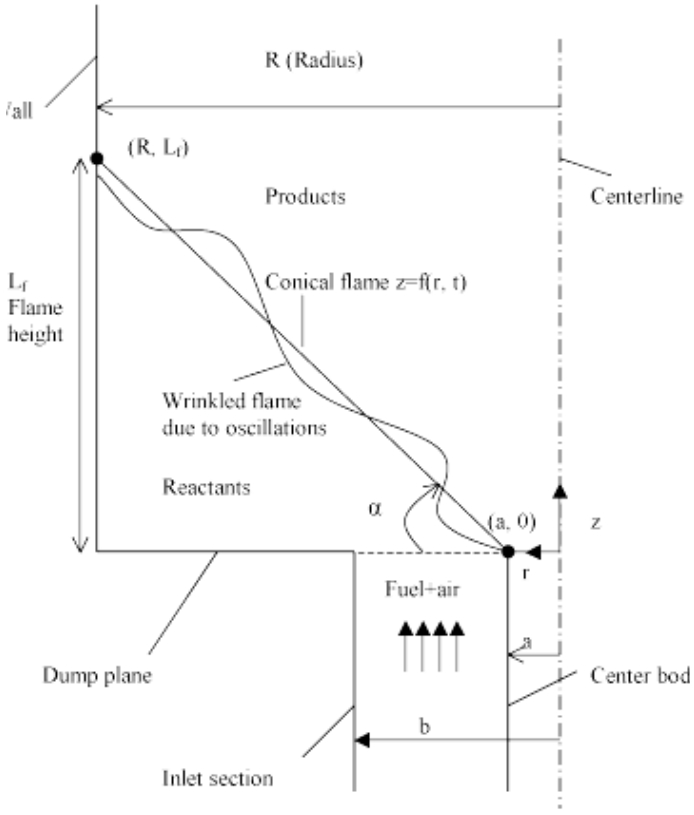

Figure 1 Geometry of the Flame

$$\frac{\partial^2 P}{\partial t^2} + c^2 \frac{\partial^2 P}{\partial x^2} = (\gamma - 1)\,\delta\left(x - x_f\right)\frac{\partial q'}{\partial t} \qquad 1$$

When solving this wave equation, fully non-reflecting and fully reflecting boundary conditions are used for closed inlet and open outlet respectively. These boundary conditions (Eq. 2-3) represent the situation inside the combustor tube realistically.

$$u'(0,t) = 0 \qquad 2$$

$$P'(L,t) = 0 \qquad 3$$

Using separation of variables technique to express pressure as the product of a time dependent amplitude $\eta(t)$ and spatial mode shape $\psi(x)$, which satisfies the boundary conditions the partial differential equation, can be simplified into an ordinary differential equation. Assuming a single dominant mode is present without any loss of generality.

$$P'(x,t) = \bar{P}\,\eta(t)\psi(x) \quad (4)$$

Similarly the acoustic velocity u' can be expressed as follows,

$$u'(x,t) = \dot{\eta}(t)\frac{\partial \psi(x)}{\partial x}k^{-2} \quad (5)$$

Plugging Eqs. 4-5 into Equation 1 we get the following ODE (Eq. 6). This is the oscillator equation that governs the acoustic behavior of the combustor.

$$\ddot{\eta} + \omega^2 \eta = \frac{(\gamma - 1)}{\bar{P}} E^{-1} \psi(x_f) \frac{dq'}{dt} \quad (6)$$

The energy E of the mode shape ψ that appears in Eq. 6 is given by Eq. 7 as follows.

$$E = \int_0^L \psi^2(x)dx \quad (7)$$

An abrupt change in the temperature thus in the speed of sound occurs before and after the flame. The change in the speed of sound needs to be accounted for in the calculation of the acoustic mode shape.

$$\rho(x) = \begin{cases} \rho_u & x \le x_f \\ \rho_d & x > x_f \end{cases}$$

$$c(x) = \begin{cases} c_u & x \le x_f \\ c_d & x > x_f \end{cases} \quad (8)$$

$$T(x) = \begin{cases} T_{in} & x \le x_f \\ T_{ad} & x > x_f \end{cases}$$

Applying the boundary conditions at the inlet and outlet along with the continuity of pressure condition across the flame interface we get the following acoustic mode shape as in the below equation.

$$\psi(x) = \begin{cases} \cos\left(\frac{\omega x}{c_u}\right) & x \le x_f \\ \frac{\cos(\alpha)}{\sin(\beta)} \sin\left(\frac{\varpi(L-x)}{c_d}\right) & x > x_f \end{cases} \quad (9)$$

In the above equation the constants α and β are defined as follows.

$$\alpha = \varpi\, x_f / c_u \quad (10)$$

$$\beta = \varpi\,(L - x_f)/c_d \quad (11)$$

Lowest possible frequency of oscillation ω is the smallest root of the following equation (Eq. 12). This shall be the dominant acoustic mode of the combustor. Other roots correspond to acoustic modes with higher frequencies. Since only one mode is assumed to be present these need not be solved for.

$$\tan\alpha \tan\beta = (\rho_u c_u)/(\rho_d c_d) \quad (12)$$

Flame Hydrodynamics. A level set based front tracking method is used to resolve flame front dynamics. Premixed flame stabilizes on the fuel injector tip, which acts like a center-body. Assuming an axisymmetric flow field and that combustion occurs on a surface whose axial position is given by a single-valued function $z = f(r,t)$, flame surface can be defined by a level-set of the well-known G-equation $G(z,r,t) = 0$. The G-equation allows one to decouple dynamics of the reacting flow field from chemistry [11].

$$G(z,r,t) = z - f(r,t) \quad (13)$$

Neglecting the radial component of velocity as both the mean and fluctuating (acoustic) component of the velocity were assumed to be one dimensional level set equation that governs, the flame front movement can be written in the following form,

$$-\frac{\partial f}{\partial t} + u = S_L \left(1 + \left(\frac{\partial f}{\partial r}\right)^2\right)^{1/2} \quad (14)$$

Since there are multiple fuels in a methane and hydrogen mixture a suitable definition of the equivalence ratio, which takes the overall stoichiometry into account is needed. Following the assumptions of Yu et. al. [12] an equivalence ratio is defined as follows (see Eq. 15). This equation implies that the hydrogen in the blend is completely oxidized and the remaining oxygen is used to burn the methane content. This is a reasonable assumption since the hydrogen oxidation proceeds much faster than methane oxidation.

$$\phi = \frac{C_{CH_4} \Big/ \left[C_{air} - C_{H_2} \Big/ \left(C_{H_2} / C_{air} \right)_s \right]}{\left(C_{CH_4} / C_{air} \right)_s} \quad (15)$$

$$S_L = \frac{C_F}{C_F + C_H} S_{L,CH_4,\phi} + \frac{C_H}{C_F + C_H} S_{L,H_2,s} \quad (16)$$

In order to solve for the flame hydrodynamics one needs to know the flame speed. For a two-fuel blend one can express flame speed as a sum of individual species' flame speed weighted by their mole fractions inside the fuel blend. Note that the flame speed of hydrogen is considered stoichiometric due to the same assumptions made for the definition of the equivalence ratio. Flame speed of methane on the other hand depends on the equivalence ratio calculated from Eq. 15. Consequently, the flame speed of the mixture is calculated using the above equation.

Experimental Setup. Numerical simulations performed are representative of the geometry and flow conditions of LSU premixed combustor. Design of this 20 kW laboratory scale combustor represents actual premixed combustor designs. Further details on the design of this combustor can be found in [14]. Figure 2 shows an overall view of the combustor and the associated longitudinal mode shape.

Figure 3 on the other hand shows a close-up view of the combustor fuel delivery section. Fuel is injected into a swirling cross flow and mixed with air before reaching the combustor dump plane. Furthermore, the injector piece acts like a center body where the tip of the conical flame is attached. Due to the small diameter of fuel injection holes the injection system has much larger acoustic impedance than the annular airflow.

Feedback Mechanism. In order to close the model it is necessary to specify a feedback mechanism between acoustic

perturbations and heat release as the rate of unsteady heat release appears on the right hand side of the oscillator

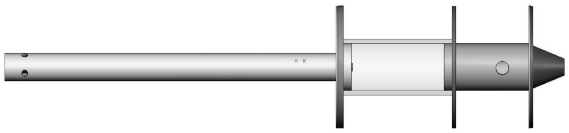

a. Combustor

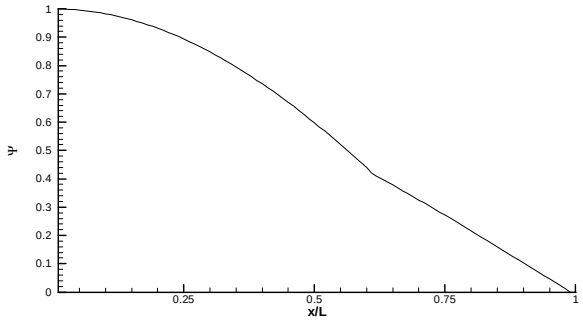

b. Mode Shape

Figure 2 Combustor and the Associated Longitudinal Mode Shape

equation. As an argument of having large impedance been made for the fuel delivery system, the fuel flow rate can be assumed steady. Consequently, variations in the airflow velocity will cause perturbations in the equivalence ratio, which will then be convected towards the flame yielding in fluctuations in the heat release. This feedback mechanism closes the loop for self-excited thermo-acoustic oscillations. Therefore, one needs to trace these equivalence ratio perturbations as they occur near the point of injection and as they are convected towards the flame zone. Another point of concern is that a fluid particle can cross the injector a number of times if the thermo-acoustic oscillations are strong enough to cause flow reversal during part of the instability cycle. Following Stow et. al. [13] equivalence ratio of a fluid particle crossing the fuel injector a number of times can be expressed mathematically as follows. In this equation Ξ denotes the set of all times when the particle crosses the axial location of the fuel injector.

$$\phi_p = \sum_{t_f \in \Xi} \bar{\phi} \frac{\bar{u}}{u(t_f)} \qquad 17$$

A fluid particle, which crosses the injector at some time $t_f \in \Xi$, does not burn instantaneously, but is convected towards the flame with the local flow velocity. For this reason the history of the particle which is currently at the flame needs to be known or be solved for analytically as in [13] if the amplitude of the limit cycle is known a priori or is being solved iteratively. In this paper an alternative approach is employed, by seeding the flow with a number of massless particles, and integrating their position in time while tracing each individual particle's equivalence ratio. Figure 4 shows the pseudo-code for tracing the particles. Note that a particle can also cross the flame interface more than once amid flow reversal. However, it can only be burned once in its first crossing of the flame interface. Therefore, if the particle currently crossing the flame has crossed it before there should be no heat released, as the fuel would have been consumed in a previous time instant. This algorithm takes care of this issue.

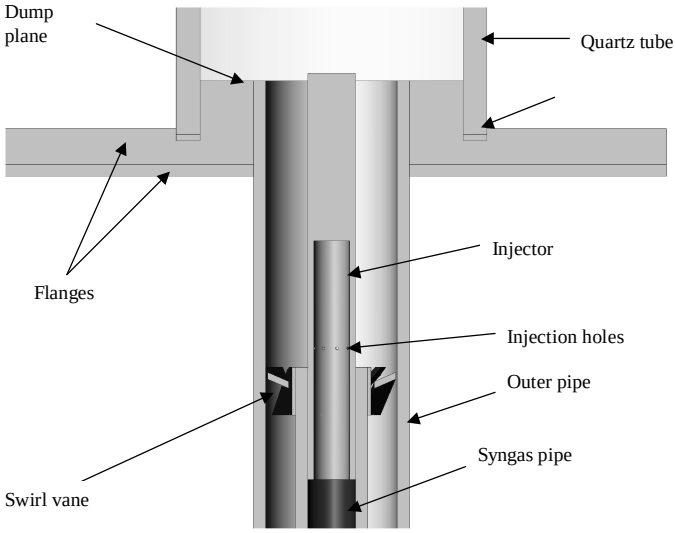

Figure 3 Detail View of the Fuel Delivery Section

$$\phi_p = \sum_{t_f \in \Xi} \bar{\phi} \frac{\bar{u}}{u(t_f)} \qquad 18$$

```
CALL InitilalizeParticles
FOR T=1 to No_of_Timesteps
CALL MoveParticles
FOR I = 1 to No_of_Particles
IF (Is_Injector_Crossed[I]=TRUE)
      Particle_ER [I] = Particle_ER_Old [I]+Ubar/U
END IF
IF (Is_Flame_Crossed [I]=TRUE)
   Is_Particle_Burned [I] = TRUE
   Particle_ER [I] = 0
END IF
IF (Is_Particle_Left_Combustor [I] =TRUE)
Particle_Position [I] = 0
Is_Particle_Burned [I] = FALSE
Particle_ER [I] = 0
END IF
END FOR
END FOR
```

Figure 4 Pseudo-Code for Tracing Equivalence Ratio of Fluid Particles

Heat Release Model. Knowing the equivalence ratio through Eq. 18 heat release can be modeled in a simplified manner as follows. Heat release per unit mass of fuel burnt can be expressed as follows as a function of equivalence ratio ϕ and heat release at stochiometric conditions Δh_s.

$$\Delta h(\phi) = \begin{cases} \phi \Delta h_s & if \quad \phi < 1 \\ \Delta h_s \; if & \phi \geq 1 \end{cases} \qquad 19$$

Furthermore, heat release q is proportional to heat release per unit mass of fuel, which is expressed in Eq. 20 as follows.

$$q(\phi) \alpha \Delta h(\phi) \qquad 20$$

Finally, knowing the amount of heat release the model can be closed and corresponding equations can be solved numerically.

RESULTS

In this section results of numerical simulations are presented. Model equations are coupled to one another and solved simultaneously. More detail for the solution is provided in [14]. For the results presented here, the inlet temperature is 300 K and the corresponding operating pressure is 1 atm. Figure 5 shows the time trace of the pressure signal between 0 to 4.1 seconds. Time trace shows an oscillatory limit cycle behavior. In the time trace occasional low frequency spikes are observed. Amplitudes of these spikes are about 7 kPa peak-to-peak.

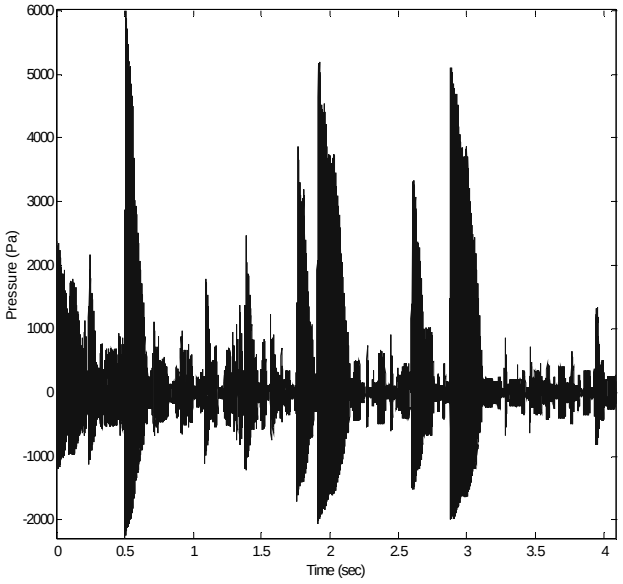

Figure 5 Time History of Pressure Signal (Q_{air}=6.2 l/s ϕ=0.9, 20% H_2 by volume)

Figure 6 shows the power spectral density of the pressure signal corresponding to the previous figure. The amplitudes are shown on a logarithmic scale. The peak at 140 Hz corresponds to the dominant frequency ω of the system. Harmonic peaks with decaying amplitudes are also observed due to the non-linearities in the dynamic model.

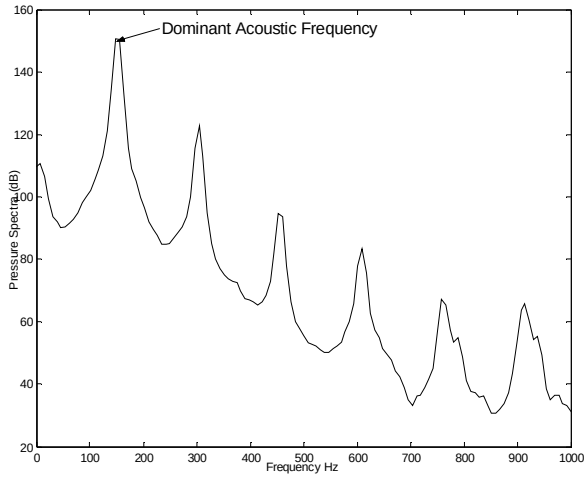

Figure 6 Power Spectral Density of the Pressure Signal (Q_{air}=6.2 l/s ϕ=0.9, 20% H_2 by volume)

Figure 7 shows the time evolution of the flame front while illustrating the flashback behavior, which is triggered by limit cycle thermo acoustic oscillations that yield in flow reversal. Position of the flame front is phase locked with respect to the pressure instability signal. Four instances with 90-degree

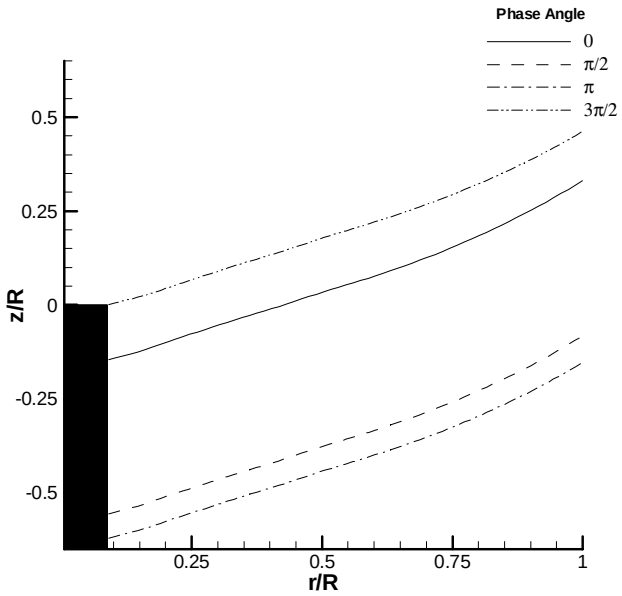

Figure 7 Time Evolution of the Flame Front Phase Locked with Pressure (Q_{air}=6.2 l/s ϕ=0.9, 20% H_2 by volume)

phase difference are shown. Owing to high frequency fluctuations flame front does not experience excessive curvature, consistent with Dowling's observations. It is seen from the figure that almost all the time flame is inside the pre-mixing section moving up and down as in the case of experiments. Only around 270-degree phase instant flame attaches the tip of the center-body (injector) briefly and de-

attaches again. During this limit cycle oscillation flame reaches its maximum propagation distance around 90-degree phase instant at which heat release is at its peak point.

Figure 8 demonstrates the effect of flow rate on RMS pressure levels. As it is seen from the graph RMS pressure level increases with increasing airflow rates. This occurs because with higher flow rates there is more fuel available to be burned inside the combustor.

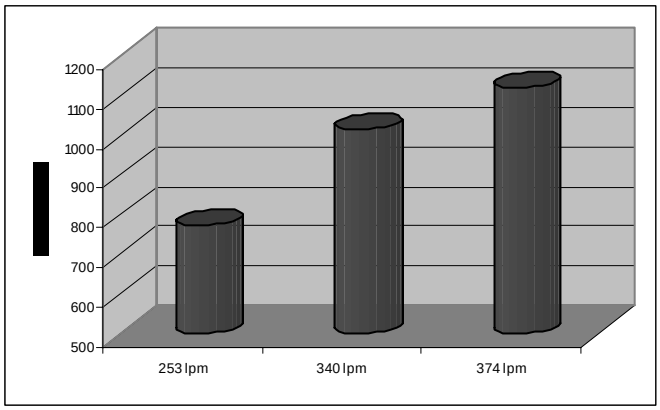

Figure 8 Effect of Flow Rate on RMS Pressure Levels (Pure CH_4, ϕ=0.7)

Finally, Figure 9 shows the effect of equivalence ratio and fuel composition on limit cycle root-mean-square pressure amplitude. With the addition of hydrogen RMS pressure levels increase over the pure methane baseline values. RMS amplitude of limit cycle pressure oscillations depend on equivalence ratio as well. It is observed that RMS amplitude is higher on the lean side and on the stoichiometric side whereas lower amplitudes were recorded in between.

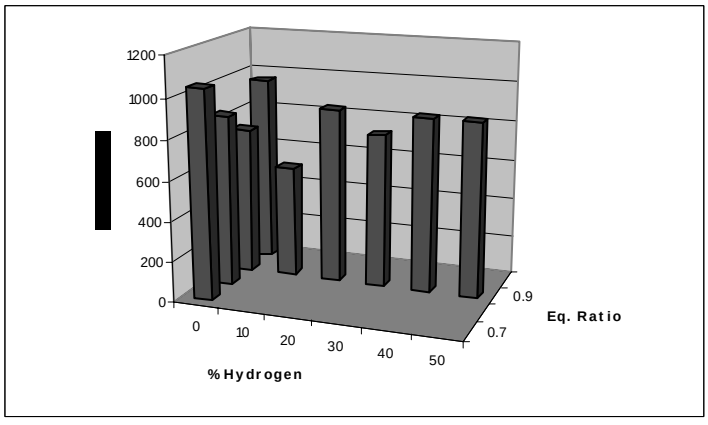

Figure 9 Effect of Equivalence Ratio and Fuel Composition on RMS Pressure Levels

CONCLUSION

A mathematical model has been developed in order to identify the thermo-acoustic instability induced flame flashback and flame holding characteristics. The following is an itemized list of main conclusions, which can be inferred from this study.

i. Non-linearity between velocity perturbations and equivalence ratio fluctuations is responsible for the limit cycle behavior. Fuel consumption effect limits the amplitude of oscillations. This effect is physical because there is only a finite amount of fuel to be burned.

ii. Amplitude of limit cycle oscillations increase with increasing flow rate. Because at higher flow rates there is more fuel available and resulting more unsteady heat release yields in more intense fluctuations in the pressure signal.

iii. Addition of hydrogen tends to increase RMS pressure levels over the baseline value with pure methane. This is consistent with the experimental observation outlined in [14].

iv. Amplitude of pressure fluctuations depend on equivalence ratio also. Amplitude increases towards the lean and stoichiometric equivalence ratios and is consequently lower in between.

Future work is aimed at using well-stirred reactor based heat release models for $CH_4/H_2/CO$ mixtures. Another challenge is to couple this model with a control algorithm. Acoustic velocities are typically an order of magnitude larger than laminar flame speeds. It is observed that flashback is primarily triggered by thermo-acoustic instability. Therefore, an active control strategy designed to suppress the amplitude of thermo-acoustic limit cycle oscillations is also anticipated to help alleviate the flashback problem.

ACKNOWLEDGMENTS

This work would never be possible without the financial support obtained from Clean Power and Energy Research Consortium (CPERC). Their support is gratefully acknowledged. I would also like to acknowledge my faculty advisor Dr. Sumanta Acharya for his encouragement and support.

REFERENCES

1. Lawn, C. J., 1999, “Interaction of the Acoustic Properties of a Combustion Chamber with Those of Premixture Supply”, Journal of Sound and Vibration, **224**, pp. 785-808
2. Dowling, A. P., 1995, “The Calculation of Thermoacoustic Oscillations”, Journal of Sound and Vibration**, 180**, pp. 557-581
3. Kiesewetter, F., Hirsch, C., Fritz, M., Kroner, M., Sattelmayer, T., 2003, “Two-Dimensional Flashback Simulation in Strongly Swirling Flows”, International Gas Turbine and Aeroengine Congress and Exposition, ASME 2003-GT-38395, Atlanta, Georgia, USA
4. Lord Rayleigh, 1896, “The Theory of Sound”, London, Macmillian
5. Tuncer, O., Acharya, S., Banaszuk, A., Cohen, J., 2003, “Side Air Jet Modulation for Control of Heat Release and Pattern Factor”, Combustion Science and Technology, ASME 2003-GT-38853, Atlanta, Georgia, USA

6. Umurhan, O. M., 1999, “Exploration of Fundamental Matters of Acoustic Instabilities in Combustion Chambers”, Center for Turbulence Research Annual Briefs, pp. 85-98
7. Smoot, L. D., Smith, P.J., 1985, “Coal Combustion and Gasification”, Plenum Press, New York, USA
8. Cowell, L. Etheridge, C., Smith, K., 2002, “Ten Years of Industrial Gas Turbine Operating Experiences”, ASME Paper No: GT-2002-30280
9. Tomzcak, H., Benelli, G., Carrai, L., Cecchini, D., 2002, “Investigation of a Gas turbine Combustion System Fired with Mixtures of Natural Gas and Hydrogen”, IFRF Combustion Journal, Article Number: 200207
10. Park, S., Annaswamy, A., Ghoneim, A., 2002, ”Heat Release Dynamics Modeling of Kinetically Controlled Burning”, Combustion and Flame, **128**, pp. 217-231
11. Markstein, G. H., 1964, “Non-Steady Combustion Propagation”, The Macmillan Company, Pergamon Press, Oxford
12. Yu. G., Law, C. K., Wu, C. K., 1986, “Laminar Flame Speeds of Hydrocarbon Plus Air Mixtures with Hydrogen Addition”, Combustion and Flame, **63**, pp. 339-347
13. Stow, S. R., Dowling, A. P., 2004, “Low Order Modeling of Themoacoustic Limit Cycles”, International Gas Turbine and Aeroengine Congress and Exposition, ASME 2004-GT-54245, Vienna, Austria
14. Tuncer, O., Uhm, J. H., Acharya, S., 2006, “Hydrogen Enriched Confined Methane Flame Behavior and Flashback Modeling”, 44th AIAA Aerospace Sciences Meeting and Exhibit, Reno, Nevada, USA, Jan. 9-12, Paper No: AIAA-2006-754